ter agreement with all the measured optical properties of smooth Na/dielectric interfaces than does the interband-transition model. It also accounts for the discrepancy between the theoretical mass and the measured mass. No doubt, interband transitions still occur in the solid, but the room-temperature optical matrix element must be much smaller than previously calculated.

Discussions with G. Graham and R. H. Silsbee have been particularly helpful. This work has been supported by National Science Foundation through Grant No. DMR-76-81083A02 to the Cornell Materials Science Center.

[1]T. Holstein, Phys. Rev. 96, 535 (1954), and Ann. Phys. (N. Y.) 29, 410 (1964).

[2]A comprehensive presentation of the alkali-metal data through 1973 has been given by P. O. Nilsson in *Solid State Physics*, edited by H. Ehrenreich, F. Seitz, and D. Turnbull (Academic, New York, 1974), Vol. 29, p. 149.

[3]R. Rouard, Thin Solid Films 34, 303 (1976).

[4]H. Mayer and M. H. el Naby, Z. Phys. 174, 289 (1963).

[5]A. W. Overhauser and N. R. Butler, Phys. Rev. B 14, 3371 (1976).

[6]J. Monin, G. Hincelin, and G. A. Boutry, C. R. Acad. Sci. Ser. B 272, 761 (1971).

[7]R. E. Palmer and S. E. Schnatterly, Phys. Rev. B 3, 2329 (1971).

[8]O. Hunderi, Phys. Rev. B 7, 3419 (1973).

[9]T. Inagaki, L. C. Emerson, E. T. Arakawa, and M. W. Williams, Phys. Rev. B 13, 2305 (1976).

[10]N. V. Smith, Phys. Rev. 183, 634 (1969).

[11]B. Hietel and H. Mayer, Z. Phys. 264, 21 (1973).

[12]When $(\omega_p\tau)^{-1} > 10^{-3}$ [for Na, $(\omega_p\tau)^{-1} \approx 7\times 10^{-3}$] a single complex frequency-dependent dielectric function can be used for all angles of incidence. K. L. Kliewer and R. Fuchs, Phys. Rev. 172, 607 (1968).

[13]N. V. Smith, Phys. Rev. B 2, 2840 (1970).

[14]D. J. Stevenson, Phys. Rev. B 7, 2348 (1973).

[15]F. S. Ham, Phys. Rev. 128, 2524 (1962).

[16]E. Burstein, W. P. Chen, Y. J. Chen, and A. Hartstein, J. Vac. Sci. Technol. 11, 1004 (1974).

[17]J. M. Elson and R. H. Ritchie, Phys. Rev. B 4, 4129 (1971).

[18]P. B. Allen, Phys. Rev. B 3, 305 (1971).

[19]*American Institute of Physics Handbook*, edited by D. E. Gray (McGraw-Hill, New York, 1972), 3rd ed.

[20]T. Inagaki, E. T. Arakawa, R. D. Birkhoff, and M. W. Williams, Phys. Rev. B 13, 5610 (1976).

Optical Detection of Magnetic Resonance for an Effective-Mass-like Acceptor in 6*H*-SiC

Le Si Dang,[a] K. M. Lee, and G. D. Watkins

Department of Physics and Sherman Fairchild Laboratory, Lehigh University, Bethlehem, Pennsylvania 18015

and

W. J. Choyke

Westinghouse Research and Development Center, Pittsburgh, Pennsylvania 15235

(Received 23 May 1980)

Optical detection of magnetic resonance is reported for the blue donor-acceptor pair luminescence in 6*H*-SiC containing nitrogen and aluminum. The nitrogen donor resonance is isotropic, with $g = 2.004 \pm 0.002$. Resonances for the aluminum acceptor in three inequivalent silicon lattice sites are detected with $g_{\parallel} = 2.412 \pm 0.002$, 2.400 ± 0.002, and 2.325 ± 0.002; and $g_{\perp} = 0$. This indicates an effective-mass-like character for the acceptor, but with reduced orbital contribution due to the localization. Evidence for corresponding reduction in the spin-orbit splitting is cited.

PACS numbers: 71.55.Fr, 71.70.Ej, 76.70.Hb, 78.20.Ls

In this Letter, we report optical detection of magnetic resonance[1] (ODMR) for the strong blue luminescence band at 2.65 eV in 6*H*-SiC doped with nitrogen and aluminum.[2] Both donor and acceptor magnetic resonances are observed, confirming that the band arises from distant donor-acceptor (DA) pair recombination.[3,4] Three distinct acceptor resonances are resolved which we identify with aluminum substituting for silicon at nonequivalent sites in the 6*H* polytype stacking sequence. The anisotropy of the resonance is characteristic of that expected from the uppermost valence-band state, indicating an effective-mass character for the Al acceptor. To our knowledge, this represents the first observation of magnetic resonance for an effective-mass-like acceptor state in any compound semiconductor, in the absence of applied uniaxial strain.[5]

ODMR experiments were carried out at 35 GHz in a TE_{011} cavity made up of concentric rings,[6] allowing large aperture for the optical beams. Magnetic fields up to 30 kG were produced by a superconducting magnet. The DA luminescence was excited with either the 350.7- and 356.4-nm lines of a Kr^+ laser or uv light from a 100-W Xe lamp. The microwave power was chopped at ~500 Hz and the corresponding synchronous changes in the luminescence intensity were observed in the direction of the magnetic field, using an RCA 4840 photomultiplier (S-20 response). Most measurements were made below the λ point of liquid helium, with the magnetic field rotating in a $(11\bar{2}0)$ plane.

Four sets of samples were used: D134, D139, D142, and D143. The increasing numbers represent sequential SiC crystal growth runs in an oven that had earlier been used for AlN crystal preparation. The Al and N impurity concentrations are estimated to be $\sim 10^{17}$–10^{18} cm^{-3} with the aluminum concentration decreasing monotonically throughout the growth series. (D134 is *p* type, D143 *n* type, a result of the decreasing aluminum concentration, trace nitrogen always being present.)

The spectral dependence of the luminescence for sample D142/GW-1 is shown in the inset of Fig. 1. The two series *B* and *C* have been interpreted[3,4] to arise from the difference in ionization energy of the donor N substituted for carbon[7] at inequivalent lattice sites. In all polytypes, the lattice sites can be classified as either of cubic (*k*) or hexagonal (*h*) local symmetry when considering the first- and second-nearest neighbors.[2] The *B* series has been assigned to nitrogen in hexagonal sites (~100 meV binding energy), and the *C* series, to cubic sites (~155 meV binding energy).[3,4] The well-pronounced peaks within each series are due to strong coupling to LO lattice phonons ~105 meV. The aluminum ionization energies have been deduced to be 239 and 248.5 meV in the hexagonal and cubic silicon sites, respectively,[3] a difference too small to be resolved in the low-temperature luminescence.

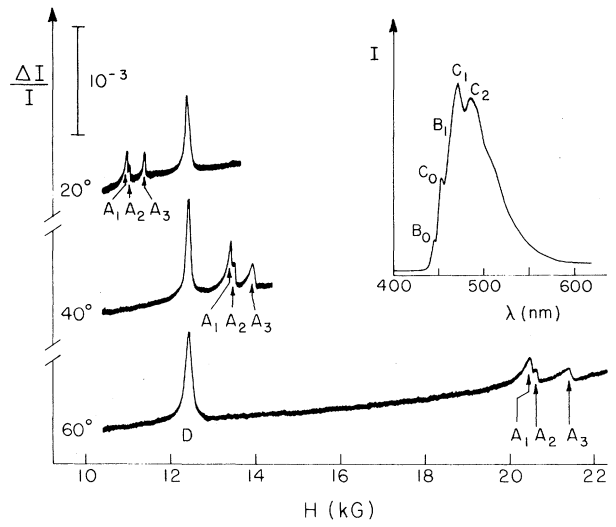

FIG. 1. ODMR spectrum in 6*H*-SiC, sample D142/GW-1, at $\nu = 34.88$ GHz, $T = 1.7$ K, for three different orientations of the magnetic field, $\theta = \cos^{-1}(\vec{H}\cdot\vec{c})$. The spectral dependence of the luminescence is shown in the inset.

Figure 1 shows the ODMR spectrum for this sample observed at 1.7 K and for several orientations of the magnetic field. The spectrum consists of one isotropic line (*D*) and a group of three resolved anisotropic lines (A_1, A_2, and A_3). Inserting a monochromator prior to the photomultiplier reveals that these ODMR lines are present throughout the complete luminescence band. We identify the isotropic line *D* as due to the nitrogen donor, the measured *g* value (2.004 ± 0.002) in good agreement with the EPR results of Woodbury and Ludwig.[8] (The small anisotropy and hyperfine interaction observed by these workers are beyond the resolution of the narrowest linewidth for *D* of ~30 G, observed in our most dilute samples.) We identify the group of anisotropic lines as due to the aluminum acceptor at nonequivalent lattice sites.

The peaks of the three ODMR transitions can be fit to the (effective spin-$\frac{1}{2}$) Zeeman expression

$$h\nu = g(\theta)\mu_B H, \tag{1}$$

where $g(\theta)$ is given by

$$g(\theta) = (g_\parallel)_i \cos\theta. \tag{2}$$

Here ν is the microwave frequency, μ_B the Bohr magneton, and θ the angle between the applied magnetic field $\vec{H}$ and the crystal *c* axis. The values for the three spectra are

$$\begin{aligned} (g_\parallel)_1 &= 2.412 \pm 0.002, \\ (g_\parallel)_2 &= 2.400 \pm 0.002, \\ (g_\parallel)_3 &= 2.325 \pm 0.002. \end{aligned} \tag{3}$$

These spectra are present in all samples studied but the closely spaced A_1 and A_2 lines are clearly resolved only in the purer crystals, where the lines are sharpest. For the 6*H* polytype there are actually two inequivalent cubic sites (k_1,k_2)

when more distant neighbors are considered.[2] One interpretation, therefore, is to assign A_1 and A_2 to the two cubic sites and A_3 to the hexagonal site. This is in the spirit of the interpretation of Ikeda, Matsunami, and Tanaka.[3] However, this is not a unique assignment. Ludwig and Woodbury, in interpreting their EPR results, equated k_2 and h as most similar because of third-neighbor similarities.[8] We conclude at this stage only that the three spectra represent inequivalent sites but assignment to specific ones must await further studies.

Let us now discuss the g factors of the acceptor. The maximum of the valence band is at the Γ point ($k=0$) in all polytypes of SiC. Recent studies of the fundamental absorption edge have been interpreted to indicate that the 6H hexagonal crystal field is larger than the spin-orbit splitting λ, which is about 7 meV for free excitons.[9] Therefore $J=L+S$ is no longer a good quantum number and the valence-band structure should be as shown in Fig. 2. The uppermost valence-band state is the doublet $(P_+\alpha, P_-\beta)$, where $P_\pm = (P_x \pm iP_y)/\sqrt{2}$ are the $L=1$ orbital states split from P_z by the hexagonal crystal field, and α, β are the spin-up and -down states, respectively. The irreducible representation of this state is Γ_9 for the $C_{6v}{}^4$ crystal group of the 6H polytype. Shown also in the figure are the corresponding labels for the C_{3v} point group of the lattice sites, the uppermost doublet being composed of $\Gamma_5+\Gamma_6$, which are degenerate because of time-reversal symmetry (Kramers degeneracy).

The Zeeman effect in this doublet can be described by

$$\mathcal{H} = \mu_B \vec{H} \cdot (g_L \vec{L} + g_S \vec{S}), \tag{4}$$

with $L=1$, $S=\frac{1}{2}$. Here, g_L and g_S are the g factors associated with the orbital angular momentum and the spin, respectively. For $g\mu_B H \ll \lambda, \Delta$, this leads to

$$g(\theta) = g_\parallel(\Gamma_9)\cos\theta; \quad g_\parallel(\Gamma_9) = 2g_L + g_S. \tag{5}$$

For the "atomiclike" case of the free hole ($g_L = 1$), Eq. (5) predicts $g_\parallel(\Gamma_9) = 4.0$. It is interesting to note, however, that in 6H-SiC, $g_\parallel$ has been observed to be systematically smaller as the hole becomes more bound: 3.2 from magneto-optic studies of the exciton bound to the neutral donor nitrogen,[10] 2.85 from similar studies for the exciton bound to the charged state of the radiation-produced CH center,[11] and, in this paper, 2.3–2.4 for the aluminum acceptor. The $\cos\theta$ angular dependence is observed in each of these cases. We interpret this to indicate that the bound hole remains effective-mass-like, reflecting the Γ_9 character of the top valence-band state, but that the orbital contribution, g_L, is progressively reduced as the hole becomes more localized. From the $(g_\parallel)_i$ values for the three acceptors, Eq. (4) gives $g_{L1} = 0.205$, $g_{L2} = 0.199$, and $g_{L3} = 0.161$. Let us now consider possible mechanisms for this orbital reduction.

One possibility is the dynamic Jahn-Teller effect. As pointed out by Morgan,[12] this may be important for bound hole states in cubic semiconductors even for small coupling strength. This should be true also in noncubic semiconductors providing that the Jahn-Teller effect is larger than the crystal field. The analysis of the DA luminescence band by Ikeda, Matsunami, and Tanaka[3] showed that the coupling to lattice vibrations is quite strong for the acceptor Al, with a Huang-Rhys factor $S \sim 1.5$ and $\hbar\omega \sim 105$ meV. Whether or not this corresponds to the Jahn-Teller coupling is not known for the present, but Huang-Rhys factors much smaller than this are sufficient to achieve this degree of reduction (see Fig. 2 of Ref. 12). The importance of the Jahn-Teller effect and the corresponding strength of the orbital reduction should depend strongly on the degree of localization because the competing elastic energy stored in the lattice decreases directly as the volume of the hole orbit.

If the dynamic Jahn-Teller effect is the mechanism, there should be a similar reduction for the spin-orbit splitting between the $\Gamma_5+\Gamma_6$ and Γ_4 states of the acceptor. We can estimate the re-

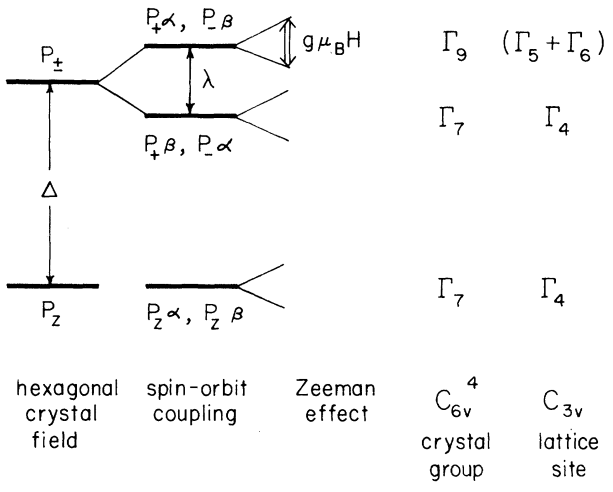

FIG. 2. The states at the top of the valence band ($k=0$).

duced values as $\lambda_i \simeq g_{Li}\lambda_0$, where $\lambda_0 \sim 7$ meV, the free-exciton value.[9] This gives $\lambda_1 \sim \lambda_2 \sim 1.4$ meV and $\lambda_3 \sim 1.1$ meV. We note that recent Raman-scattering studies in the aluminum-doped 6*H*-SiC have detected zero-field transitions at 1.50, 1.32, and 1.12 meV.[13] These were tentatively assigned to exciton exchange splittings at titanium impurities, known to be of this magnitude, even though no titanium bound-exciton luminescence was observed under the conditions of the experiment. Our present results suggest that the correct origin for these transitions is the reduced spin-orbit splitting at the neutral aluminum acceptors. The close agreement with our predicted values lends support to the dynamic Jahn-Teller origin for the orbital reduction. (The spin-orbit splitting of 4.8 meV observed for the exciton bound to neutral nitrogen[14] also fits this model well.)

Other mechanisms could also be important. The relative magnitude and sign of the contributions to the orbital matrix elements from atoms on each of the various sublattice shells surrounding the aluminum center could depend critically on the degree of localization.[15,16] In this case, changes in λ would also occur, but, considering the differing contributions from the silicon and carbon atomic spin-orbit couplings, they would not necessarily be related to the orbital reduction by a simple factor.[17]

In conclusion, we have detected both the distant nitrogen donors and aluminum acceptors by ODMR for the ~2.65-eV DA luminescence band in 6*H*-SiC. Three distinct acceptor resonances have been resolved which we interpret as arising from aluminum atoms on inequivalent silicon sites in the polytype stacking sequence. The anisotropy of the acceptor resonances is characteristic of the uppermost Γ_9 valence-band hole state but with reduced orbital angular-momentum contributions resulting from the localization. A dynamic Jahn-Teller origin for this reduction predicts a corresponding reduction in the spin-orbit interaction. Confirmation of this is provided by a new interpretation of the recent Raman-scattering studies of Scott, Toms, and Choyke.[13]

In the common cubic compound semiconductors, the *p*-like character and degeneracy of the top of the valence band make effective-mass-like hole states very sensitive to random strains. The magnetic resonance lines are therefore very broad and difficult to detect. In the results reported here, the built-in crystal field of the hexagonal-SiC polytypes has served the vital role of lifting this degeneracy, making the observation of hole states possible. Another example of this situation is GaSe for which ODMR of the free hole has been recently reported.[18] Further studies of acceptor states in compound semiconductors would profit by studying hexagonal polytypes.

The authors acknowledge helpful discussions with W. Beall Fowler, F. S. Ham, and T. N. Morgan. This research was supported by the National Science Foundation under Grant No. DMR-77-11309.

---

[a]Permanent address: Laboratoire de Spectrométrie Physique, B.P. 53, F-38041 Grenoble, France.

[1]For a review of ODMR applied to semiconductors, see B. C. Cavenett, J. Lumin. 18/19, 846 (1979).

[2]For a recent review on the properties of SiC, see Y. M. Tairov and Y. A. Vodakov, in *Electroluminescence*, edited by J. I. Pankove, Topics in Applied Physics Vol. 17 (Springer-Verlag, Berlin, 1977), p. 31.

[3]M. Ikeda, H. Matsunami, and T. Tanaka, J. Lumin. 20, 111 (1979).

[4]A. W. C. Van Kemenade and S. H. Hagen, Solid State Commun. 14, 1331 (1974).

[5]EPR of acceptors in GaAs was observed by applying uniaxial stress by R. S. Title, IBM J. Res. Dev. 7, 68 (1963).

[6]M. Chamel, R. Chicault, and Y. Merle d'Aubigné, J. Phys. E 9, 87 (1976).

[7]The identification of the sublattice on which nitrogen and aluminum substitute comes from reference to boron which is known to substitute for carbon from EPR studies [H. H. Woodbury and G. W. Ludwig, Phys. Rev. 124, 1083 (1961)]. Resolved DA spectra for N-B close pairs reveal them to be on the same sublattice (type-I spectrum) [S. Yamada and H. Kuwabara, in *Silicon Carbide 1973*, edited by R. C. Marshall, J. W. Faust, Jr., and C. E. Ryan (Univ. of South Carolina Press, Columbia, 1974), p. 305]. Similar studies for the N-Al system reveal them to be on different sublattices (type-II spectrum) {W. J. Choyke and L. Patrick, Phys. Rev. B 2, 4459 (1979); N. N. Long, D. S. Nedzvetskii, N. K. Prokofeva, and M. B. Reifman, Opt. Spektrosk. 29, 727 (1970) [Opt. Spectrosc. (USSR) 29, 388 (1970)]}.

[8]Woodbury and Ludwig, Ref. 7.

[9]R. G. Humphreys, D. Bimberg, and W. J. Choyke, to be published.

[10]P. J. Dean and R. L. Hartman, Phys. Rev. B 5, 4911 (1972).

[11]W. J. Choyke, L. Patrick, and P. J. Dean, Phys. Rev. B 10, 2554 (1974).

[12]T. N. Morgan, Phys. Rev. Lett. 24, 887 (1970).

[13]J. F. Scott, D. J. Toms, and W. J. Choyke, Phys. Rev. B 21, 3432 (1980).

[14]W. J. Choyke and L. Patrick, Phys. Rev. 127, 1868 (1962).

[15]D. Y. Smith, Phys. Rev. B 8, 3939 (1973).
[16]D. Bimberg and P. J. Dean, Phys. Rev. B 15, 3917 (1977).
[17]D. Y. Smith, Phys. Rev. B 6, 565 (1972).
[18]K. Morigaki, P. Dawson, and B. C. Cavenett, Solid State Commun. 28, 829 (1978).

Noncompact σ Models and the Existence of a Mobility Edge in Disordered Electronic Systems near Two Dimensions

A. Houghton, A. Jevicki, and R. D. Kenway
Department of Physics, Brown University, Providence, Rhode Island 02912

and

A. M. M. Pruisken
Institute für Theoretische Physik, Universität Heidelberg, D-6900 Heidelberg, Germany

(Received 17 April 1980)

The properties of an electron in a disordered solid are discussed with use of a matrix nonlinear σ model first introduced by Wegner and Schäfer. The model is defined on the noncompact space $O(M,M)/[O(M)\times O(M)]$ where M is the number of replicas. This noncompact symmetry represents the essential physics of the problem. It is found that all states are localized in two dimensions; above two dimensions for weak disorder there are mobility edges, but these merge above a critical amount of disorder and all states become localized.

PACS numbers: 71.55.Jv, 11.10.Gh, 11.10.Lm

The electronic properties of a disordered solid may be described by the Hamiltonian[1,2]

$$H=\frac{1}{\sqrt{n}}\sum_{\substack{\vec{r},\alpha\\ \vec{r}',\alpha'}}|\vec{r},\alpha\rangle f_{\vec{r},\alpha;\vec{r}',\alpha'}\langle\vec{r}',\alpha'|\ ; \tag{1}$$

at each site $\vec{r}$ of a regular lattice, spacing a, there are n orbitals α. On-site energies and inter-site hopping are randomly distributed. Here we will take $\underline{f}$ to be a real symmetric matrix. In a series of interesting papers it was first conjectured[3] and then proved[4] that the properties of the system described by Eq. (1) may be discussed in terms of a field theory with action[5]

$$\begin{aligned}&A=\tfrac{1}{2}K\int d^dx\ \mathrm{Tr}[\partial_\mu V(x)][\partial_\mu V(x)],\\ &\underline{V}^2=\pm\lambda_0{}^2\underline{1},\end{aligned} \tag{2}$$

where (Refs. 2 and 4) $K=nR^2a^{-d}/4d$ and $\lambda_0=(1-E^2/E_0{}^2)^{1/2}$. This action arises on averaging a product of single-particle Green's functions $G(\vec{r},\vec{r}',z_p)$, $p=1,2$ over the distribution of the matrices $\underline{f}$.[4] It is defined on a set of real symmetric matrices, $\underline{V}^2=\lambda_0{}^2\underline{1}$, if the two energies lie on the same side of the real axis. However, in the case of most interest, the conductivity, the energies, z_p, lie on opposite sides of the real axis and a model of complex symmetric matrices, $\underline{V}^2=-\lambda_0{}^2\underline{1}$ results. This difference reflects the distinct symmetries of the two cases. In the first case, the system is invariant under orthogonal transformations and the matrices $\underline{V}$ are elements of the compact space $O(2M)/[O(M)\times O(M)]$ where M is the number of replicas in the spaces $p=1$ and 2. For the conductivity, the symmetry is hyperbolic and the fields belong to the noncompact space $O(M,M)/[O(M)\times O(M)]$.

In Ref. 4 it was argued that at the level of perturbation theory the two models are equivalent and therefore the critical properties in the hyperbolic case, namely the behavior of the electronic system near a mobility edge, could be described by the generalized compact nonlinear σ models

$$\begin{aligned}&A=(1/2t_0)\int d^dx\ \mathrm{Tr}[\partial_\mu g^{-1}(x)][\partial_\mu g(x)],\\ &\underline{g}^2=\underline{1},\quad \underline{g}\in O(2M)/[O(M)\times O(M)],\end{aligned} \tag{3}$$

discussed previously by Brézin, Hikami, and Zinn-Justin.[6] In this Letter we will point out the important difference between the compact and noncompact models in a $2+\epsilon$ expansion. As we shall see, it is precisely this difference which represents the essential physics of the mobility-edge problem.

First, we note that the action Eq. (2) for $\underline{V}^2=-\lambda_0{}^2\underline{1}$ can be written in terms of real matrices $\underline{g}$ as

$$\begin{aligned}&A=-(1/2t_0)\int d^dx\ \mathrm{Tr}[\partial_\mu g^{-1}(x)][\partial_\mu g(x)],\\ &\underline{g}^2=\underline{1},\quad \underline{g}\in O(M,M)/[O(M)\times O(M)],\end{aligned} \tag{4}$$